A unified model to predict the hot stamping and subsequent stress-relaxation process of a Ti-6Al-4V alloy

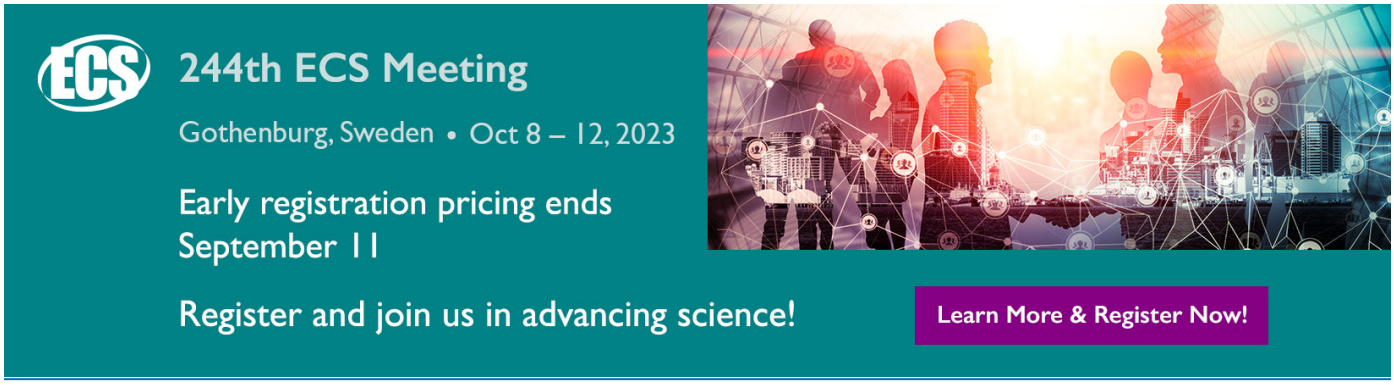

A unified model to predict the hot stamping and subsequent stress-relaxation process of a Ti-6Al-4V alloy

H S Chen[1], **L H Du**[2], **M Shahzad Khan**[1], **T Zhang**[2], **Y H Mu**[2], **Y Zhang**[1] **and Y Li**[1,3,*]

[*] Corresponding author, E-mail: liyong19@buaa.edu.cn

[1] School of Mechanical Engineering and Automation, Beihang University, Beijing, 100191, P.R. China

[2] AVIC Manufacturing Technology Institute, Beijing, 100024, P.R. China

[3] Shenzhen Institute of Beihang University, Shenzhen, 518057, P.R. China

[*] Corresponding author, E-mail: liyong19@buaa.edu.cn

Abstract. Isothermal hot stamping process, which is composed of stamping and subsequent stress-relaxation steps, is an important technology to form complex thin-walled titanium components in the aerospace industry. It is a key issue to enable the accurate simulations of these two steps simultaneously for the process design and optimization. In this study, a unified constitutive model connecting both the plastic flow behaviour in stamping and the stress-relaxation behaviour in subsequent step is developed by considering the continuous evolution of key microstructures, i.e., dislocation density, in the whole process. A series of basic mechanical tests, including tensile and stress-relaxation tests, of a typical titanium alloy Ti-6Al-4V at 750°C was performed to calibrate the developed model. The unified model was then implemented into the commercial software ABAQUS via the VUMAT subroutine, and simulations of the complete hot stamping process were done, including stamping, stress-relaxation and final springback. In addition, a typical curve-shape component was hot-stamped at 750°C and stress-relaxation for 5 minutes was performed. The predicted result from the developed constitutive model and FE model shows a good agreement of the springback with the corresponding experimental result, verifying the effectiveness of the developed model for the further applications in hot stamping process design and optimization in the industry.

Keywords. hot stamping, stress-relaxation, Ti-6Al-4V, constitutive model, springback

1. Introduction

The high strength and lightweight titanium alloys are widely used in aerospace industry for thin-walled structural components. Hot forming technologies are required for titanium alloys to gain acceptable forming force and formability. Up to now, many hot forming technologies of titanium alloys have been developed, such as isothermal hot stamping, cold-die hot stamping [1], creep forming and superplastic forming [2]. Isothermal hot stamping, due to its advantages in formability, forming accuracy and low residual stress, has been widely used in the production of aviation products.

A typical isothermal hot stamping process is generally composed of 4 steps, as illustrated in figure 1, including: 1) heating the die and sheet blank to the forming temperature; 2) stamping the blank into the desired shape; 3) holding the mould for several minutes to do stress-relaxation and minimize springback; 4) release the mould and final springback of the formed product occurs. In the whole process, both stamping and stress-relaxation steps, governed by plastic flow and stress-relaxation behaviour of materials respectively, are critical to determine the shape accuracy of the formed products.

Hence, it is a key issue to enable the accurate simulation of these two steps simultaneously for the process design and optimization.

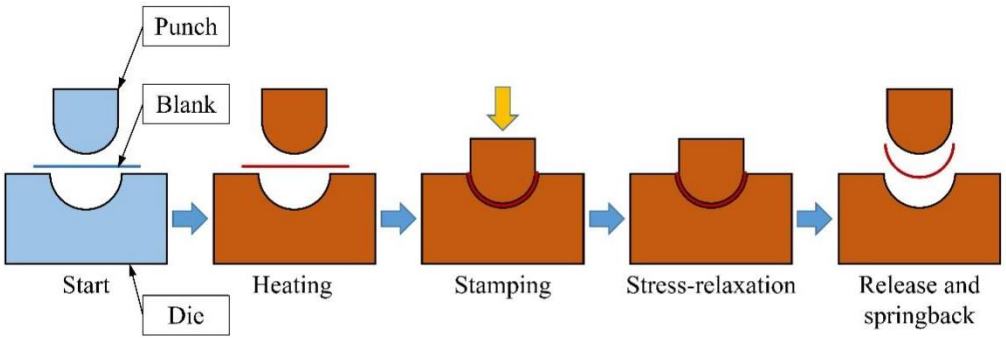

Figure 1. Schematic of typical isothermal hot stamping process.

For the plastic deformation behaviour dominated in the stamping step, both phenomenon-based and mechanism-based models are developed. Johnson-Cook model, as one of the most widely used rate-dependent phenomenon-based empirical model, has been modified and implemented to predict the flow behavior of Ti–6Al–4V at temperatures ranging from room temperature to 1100°C, with strain rate up to 10^3/s [3,4]. Arrhenius model has also been proved to be successful in the predicting of stress-strain response of Ti-6Al-4V [5]. Deformation mechanisms, such as work hardening and dynamic recrystallization, have been adopted into constitutive models as state variables by Porntadawit et al. [6]. Lin et al. [7,8] further developed a set of mechanism-based unified constitutive models to include the mechanism-controlled microstructural variables, enabling the successful modelling of the viscoplastic behaviour of aluminium alloys and titanium alloys at high temperature [9–12].
For the stress-relaxation behaviour dominated in the stress-relaxation step, logarithmic expressions, exponential expressions, hyperbolic laws and Maxwell delay functions are often used for corresponding modelling. The mechanism of stress-relaxation is creep, of which the essence is the transition of elastic strain into plastic one while the total strain remain unchanged [13]. Xiao et al. [14] have used an explicit delay function and an implicit hyperbolic law to model the creep behavior of Ti-6Al-4V with temperatures ranging from 650°C to 750°C respectively. Effect of microstructures on the creep process of Ti-6Al-4V has been studied by Luo et al. [15] and Arrhenius and Norton equations have been used to describe the variation of stresses during the process. Moreover, a series of mechanism-based creep models on the basis of the unified theory [7,8], considering the hardening mechanism and microstructure evolution, has been developed recently to predict the different stress-relaxation ageing behaviours with elastic and plastic initial strains [16–18].
Although individual models have been developed for either step, for the isothermal hot stamping with continuous stamping and stress-relaxation steps, a unified model to combine these two steps for the accurate simulation of springback is still lacking. The transmission of material states between two steps and the continuity of constitutive models are major challenges.
Hence, the main purpose of this study is to propose a model to predict the continuous stress and microstructure evolutions in the complete isothermal hot stamping process. Microstructure such as dislocation and cavity damage are considered in this model, and dislocation density act as medium to transmit material state between two steps. This model can present accurate results for the simulation of isothermal hot stamping or other processes that experience similar procedure, and provide direct suggestions for further process optimization.

2. Material tests and constitutive model

The tensile tests and stress-relaxation tests were performed to get the detailed plastic flow and creep behaviours of Ti-6Al-4V. Based on which, a dislocation based unified constitutive model is developed to describe the continuous evolutions of both microstructures and mechanical properties during stamping and subsequent stress-relaxation steps.

2.1. Material and test programme

The material used is the TC4 (Ti-6Al-4V) titanium alloy sheet, provided by BAOTI Group, with a fine equiaxed grains. The material composition is listed in table 1.

Table 1. Composition of TC4 titanium alloy.

Ti	Al	V	Fe	C	N	H	O
Balance	6.02%	3.92%	0.05%	0.02%	0.02%	0.004%	0.12%

The uniaxial tensile tests were performed at 750°C on ZWICK/Roll-Z100 testing machine according to GB/T 228.2-2015, with strain rate 0.10/s, 0.033/s and 0.01/s respectively. The experimental result is plotted in figure 5. The stress-relaxation tests were performed on RWS-50 creep relaxation tester according to GB/T10120-2013. The specimen was stretched to pre-strain and held, and the load values versus time are recorded. The pre-strain is selected as 5% and stress-relaxation time is 1800s.

2.2. Development of material model

The model developed in this study composed of two parts: model for plastic deformation and model for stress-relaxation. Although the process is divided into two steps, the microstructure evolution in this process, such as dislocation density, is changing continuously and therefore can be used as a critical state variable linking the two steps. Thus, a set of unified constitutive models for these two steps is developed through the continuous simulation of microstructural evolutions under different loading states.

2.2.1. Dislocation density evolution model. It is generally accepted that the plastic deformation and creep deformation of titanium alloys in hot stamping conditions are mainly dominated by the motion and evolution of dislocations, and hardening or softening is also associated with interaction of dislocations [19]. The dislocation density evolution at high temperature mainly includes dislocation accumulation, static recovery and dynamic recovery [7], which are very similar in stamping step and stress-relaxation step. Thus, the dislocation density evolution of the two steps can be expressed by the same formula to enable the continuity of the microstructure evolutions. Considering the time scale of hot stamping and stress-relaxation are several minutes and strain is usually not very large, which are insufficient to produce significant recrystallization [20], only the static and dynamic recoveries are considered in the dislocation density evolution equation in this study. Evolution equation of the normalized dislocation density $\bar{\rho}$ for the whole process is proposed as followed [7,10]:

$$\dot{\bar{\rho}} = A_2(1-\bar{\rho})|\dot{\varepsilon}| - C\bar{\rho}^{n_2} \quad (1)$$

The first term in equation (1) represents dynamic recovery and the accumulation of dislocations due to plastic or creep deformation (both represented by ε here); the second term represents the static recovery of dislocations [18]. A_2, C in this equation are temperature dependent parameters, n_2 is material constant. $\bar{\rho}$ is defined by $\bar{\rho} = (\rho - \rho_0)/(\rho_{max} - \rho_0)$, where ρ_0 is the initial dislocation density, ρ is the instantaneous dislocation density and ρ_{max} is the maximum dislocation density in the whole process.

The Taylor equation modelling the dislocation hardening R is given as followed [10]:

$$R = B_2\bar{\rho}^{0.5} \quad (2)$$

B_2 is a temperature dependent parameter. In the unified model, the result of dislocation density evolution during stamping step is transmitted into stress-relaxation step and act as the initial state of stress-relaxation, realizing the inheritance of microstructure between two steps.

2.2.2. Plastic deformation model for hot stamping step. To model the viscoplastic behavior, the widely accepted Perzyna viscoplastic model describing the relationship between plastic strain rate $\dot{\varepsilon}^p$ and stress σ is used, as follows:

$$\dot{\varepsilon}^p = \langle \frac{\sigma/(1-\omega) - R - k}{K} \rangle^{n_1} \quad (3)$$

The term $(\sigma/(1-\omega) - R - k)$ is the stress that leads to viscoplastic flow [21]. Plastic deformation, dislocation density evolution and cavity damage occur only when this term is greater than zero. σ in this term means loading stress and k represents yield stress. K in this equation means viscosity parameter and is temperature dependent. The output of this function, $\dot{\varepsilon}^p$, is the plastic strain rate.
ω in equation (3) means damage factor, which represents microstructure damage evolution, and is defined in equation (4). Material failure is defined to occur when ω is greater than 0.7 [12]. η_1, η_2 are temperature dependent parameters and η_3 is material constant.

$$\dot{\omega} = \frac{\eta_1 \sigma}{(1-\omega)^{\eta_2}} (\dot{\varepsilon}^p)^{\boldsymbol{\eta_3}} \quad (4)$$

2.2.3. Creep model for stress-relaxation step. A hyperbolic law equation (5) with the $sinh$ function is used to model the creep strain evolution in this study. The $\bar{\rho}$, R and k are exactly the same as they are in the stamping model. When the term in the $sinh$ function equal to zero, the creep behavior stop and the stress value at this critical level is defined as threshold stress.

$$\dot{\varepsilon}^c = A_1 \, sinh\left\{B_1\left[|\sigma|\left(1-\bar{\rho}\right) - m(R+k)\right]\right\} \quad (5)$$

2.2.4. The unified constitutive model. Based on the equations listed above, a full set of unified constitutive models considering a continuous evolution of dislocation density between different steps of plastic deformation and stress-relaxation can be developed, which is summarised in table 2. The dislocation density evolution functions are identical in two steps, which means the microscopic mechanism is unified in both steps and the microstructure change caused by loading history can be transmitted into the stress-relaxation model.

Table 2. The unified constitutive model for isothermal hot stamping process.

	Model for plastic deformation	Model for stress-relaxation
Stress update at each step	$\sigma = E(1-\omega)(\varepsilon - \varepsilon^p)$	$\dot{\sigma} = -E\dot{\varepsilon}^c$
Strain response at each step	$\dot{\varepsilon}^p = \langle \frac{\sigma/(1-\omega) - R - k}{K} \rangle^{n_1}$	$\dot{\varepsilon}^c = A_1 sinh(\{B_1[\lvert\sigma\rvert(1-\bar{\rho}) - m(R + k)]\})$
Continuous dislocation density	$\dot{\bar{\rho}} = A_2(1-\bar{\rho})\lvert\dot{\varepsilon}\rvert - C\bar{\rho}^{n_2}$	
Continuous dislocation hardening	$R = B_2\bar{\rho}^{0.5}$	
Damage factor	$\dot{\omega} = \frac{\eta_1 \sigma}{(1-\omega)^{\eta_2}} (\dot{\varepsilon}^p)^{\boldsymbol{\eta_3}}$	

3. Hot stamping test and FE simulations

To verify the accuracy of the developed material model, a curved part made by TC4 material was formed and scanned into 3D model as a standard reference. A series of FE simulations of this part were built based on the constitutive model developed in this study.

3.1. Hot stamping test

An isothermal hot stamping test was performed to produce a curved part. The thickness of the blank was 1.5mm. The picture of die and punch are shown in figure 2, with the stamping clearance 1.1 times the thickness of the sheet. The stamping was performed at 750℃, with a stamping speed of 1.5mm/s and the stamping process took 65 seconds to complete. After stamping, the whole set of instruments was held for 5 minutes, and then the workpiece was released. The shape of the stamped part was scanned into point cloud data by FreeScan X3 scanner for further comparisons.

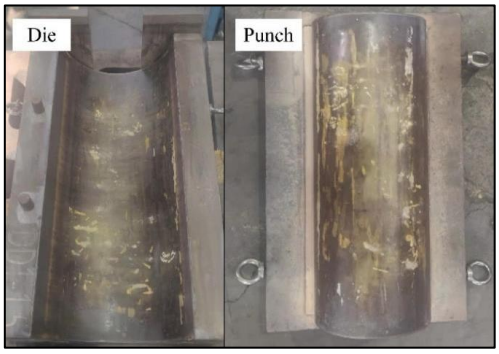

Figure 2. Hot stamping mould.

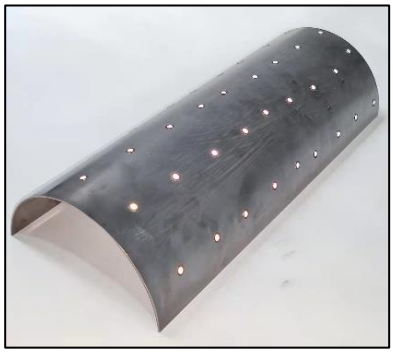

Figure 3. Curved part after isothermal hot stamping.

3.2. FE simulation model

A simulation case for forming this part was built in commercial finite element software ABAQUS. The blank had a length of 490mm and a width of 302mm. The diameter of the semi-circular surface for punch and die were 191.85mm and 195.15mm respectively. The punch and die were meshed in rigid elements and the blank in S4RT shell unit. The minimum size for elements was 3 mm. The number of thickness integration points was 7. The FE model of this part can be seen in figure 4.

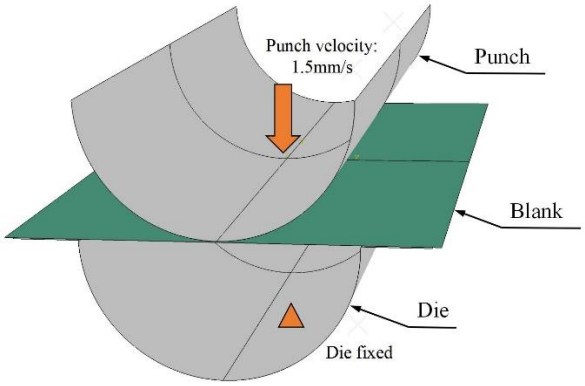

Figure 4. FE model of hot stamping.

Some basic properties such as density and thermal conductivity were defined in material module, as listed in table 3 [22]. The elastic modulus was derived from uniaxial tensile test data fitting. The constitutive model listed in table 2 were implemented into stamping step and stress-relaxation step by two VUMAT subroutines respectively. Dislocation density and cavity damage were defined as solution-dependent state variables, which were passed through the predefined field in two steps.

Table 3. Basic material properties of TC4 at 750℃.

Density (tonne/mm^3)	4.4E-9
Elastic modulus (MPa)	38455.6
Poisson ratio	0.39
Conductivity (mW/(mm · K))	16.41
Specific Heat (mJ/(tonne · K))	7.23E+8

For boundary conditions, the whole set of instruments was given a temperature of 750℃ during all steps, other boundary conditions are listed in table 4. Punch and die were removed from the model after the stamping step. Coefficient of friction between moulds and blank was set as 0.1.

Table 4. Boundary conditions at each step.

Step	Stamping	Stress-relaxation	Springback
Punch	Move toward die at 1.5mm/s	Removed	Removed
Die	Fixed	Removed	Removed
Blank	--	Fixed	3 points support

The whole simulation process was divided into three analysis steps. The stamping step and stress-relaxation step were firstly calculated by thermodynamic coupled explicit analysis. Then the result was transmitted into implicit analysis by using predefined field. Springback was then performed using coupled temp-displacement implicit analysis.

4. Result and discussion

4.1. Hot deformation and stress-relaxation behaviour under different conditions

4.1.1. Calibration of the constitutive model. The constitutive equations in this study are presented implicitly in the form of differential equations. Stress-strain data obtained by uniaxial tensile test and stress-time data obtained from hot stress-relaxation test are used to fit the material parameters of two steps respectively. Genetic algorithm has been proved to be effective in calibration of the constitutive model [23,24] and is used in this study. The calibration result for TC4 material in 750℃ is shown in table 5.

Table 5. Material constant for unified model of TC4 at 750℃.

Model for plastic deformation		Model for stress-relaxation	
k(MPa)		2.3457E+01	
A_2		2.7472E+02	
n_2		2.5452E+00	
B_2(MPa)		1.1631E+02	
$C(\mathrm{s}^{-1})$	1.1372E+00	$C(min^{-1})$	1.8954E-02
K(MPa)	4.7689E+02	$A_1(min^{-1})$	1.9088E-03
n_1	2.9638E+00	$B_1(MPa^{-1})$	6.3364E-02
$\eta_1(\mathrm{MPa}^{-1})$	1.1454E-03	m	2.1094E-02
η_2	6.6908E+00		
η_3	1.0602E+00		

4.1.2. Constitutive model results and discussion. The constants in table 5 are used to predict the stress response during the loading step, which is shown in figure 5. The symbols in figure 5 show the tensile test results for TC4 at 750℃ under different strain rates and the solid lines are the predicted results for corresponding cases, which demonstrate a good agreement between the model predictions and experimental results for all the 3 different strain rates. Figure 6(a) shows the predicted results for dislocation density evolutions. At every strain rate level, dislocation density increases steadily due to plastic deformation and then reach an equilibrium state, which means that the dislocation density accumulation rate due to plastic deformation is equivalent to the rate of static recovery. At higher strain rate level, a higher dislocation density is needed to accelerate the static recovery to balance the accumulation of dislocation density. Figure 6(b) presents the relations between the damage and strain for different strain rate conditions. Cavity damage increases steadily in the early stage and rapidly in the late stage, resulting in the softening section of the stress-strain curves. The high flow stress caused by the high strain rate accelerates the damage growth of the material, resulting in the reduction of the ultimate strain.

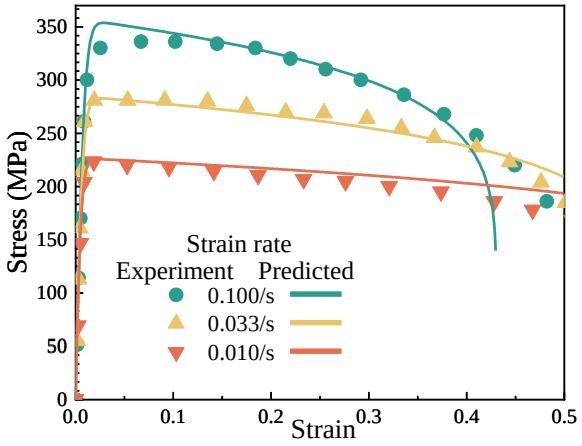

Figure 5. Experimental and predicted flow stress of TC4 at 750℃ under different strain rates.

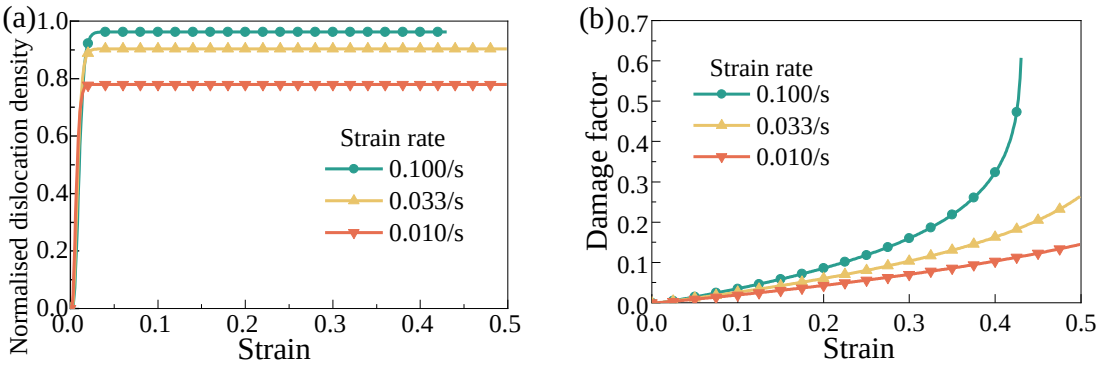

Figure 6. Predicted (a) normalised dislocation density and (b) damage factor evolution of TC4 at 750℃ under different strain rates.

Then a complete load and stress-relaxation process is calculated by the model given above, which composed of a plastic deformation step and a subsequent stress-relaxation step, and the stress response is plotted in figure 7(a). It can be found that the stress-relaxation rate of TC4 is pretty fast: most of the stress can be relieved in 10 minutes, and the stress is close to the steady state at 15 minutes. The evolution of dislocation density is shown in figure 7(b). At the primary relieve stage, dislocation density grows rapidly due to high creep strain rate and then decreases as the residual stress drops. At the steady relieve stage, the static recovery plays a leading role in the evolution of dislocation, and drive the dislocation density to decrease gradually.

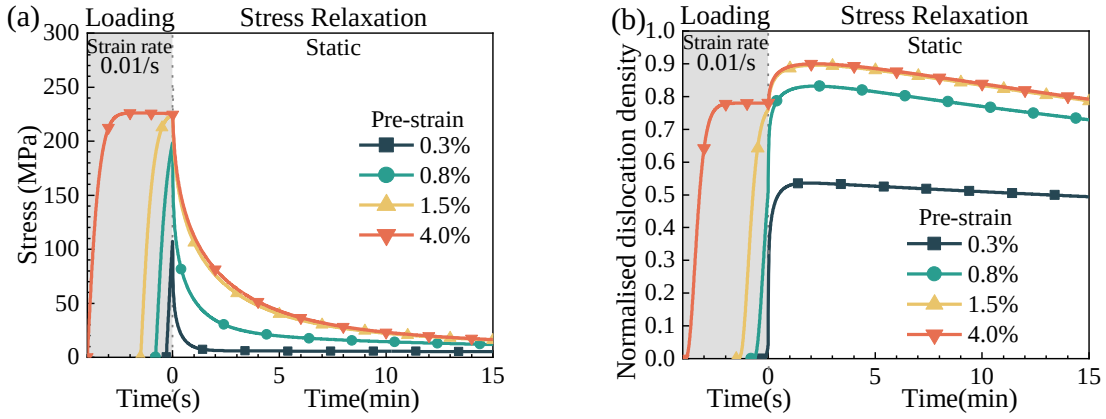

Figure 7. Predicted (a) stress and (b) normalised dislocation density evolution of a continuous load and stress-relaxation process of TC4 at 750℃ under different pre-strain.

4.2. Residual stresses and springback after isothermal hot stamping

The unified constitutive model is implemented into FE analysis and simulation results are obtained. The surface stress (Von Mises stress at the bottom surface of the blank) distributions during the whole stamping procedure are shown in figure 8. It is observed that some stress decline occurs during the stamping step. This phenomenon can be attributed to two factors. The first one is the reduction of elastic strain. As the loading process is very slow, the total strain rate in the later stage of loading decreases to an extremely small level (1E-4/s to 1E-5/s), while the plastic strain rate from equation (3) would experience a slower decreasing speed as the applied stress remains. When the plastic strain rate is higher than the total strain rate, reduction of elastic strain occurs, leading to the relaxation of stresses. The second one is due to the continuous static recovery behavior during the comparatively long-term stamping step of 65 seconds.

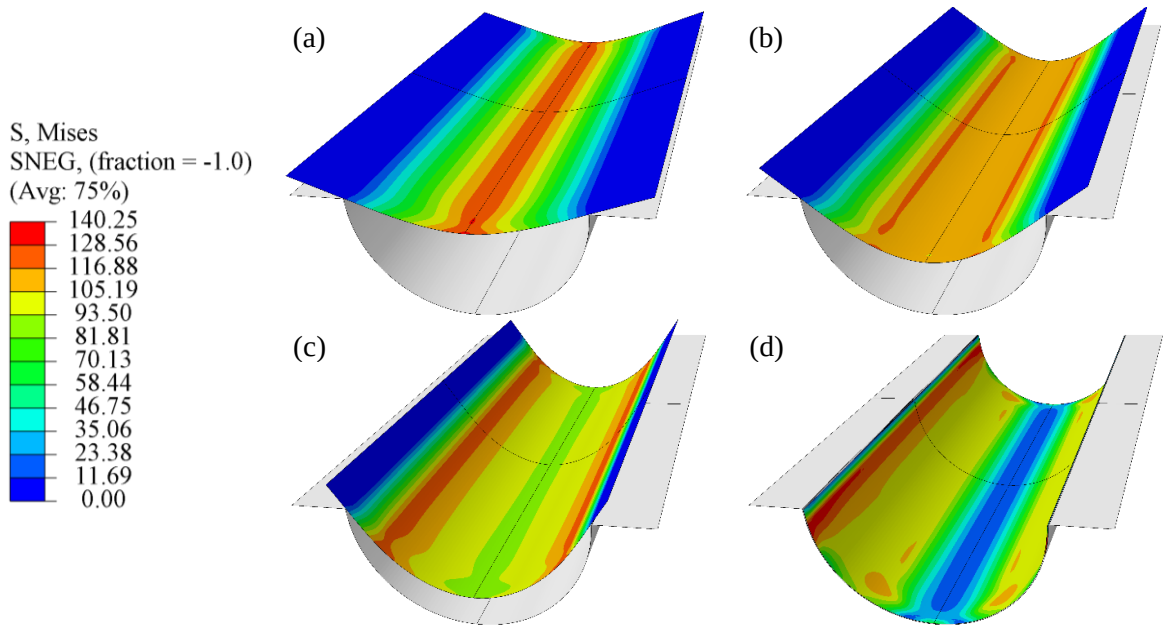

Figure 8. Surface stress distribution in the stamping part at (a) 25%, (b) 50%, (c) 75% and (d) 100% of stamping stroke.

Figure 9 shows the stress variation during the stress-relaxation and springback steps. An apparent relaxation of stress is observed during stress-relaxation, with the initial stress values of 13.20MPa to 138.96MPa to the final values of only 1.42MPa to 10.74MPa after 5 minutes. Through stress-relaxation treatment, the range and average value of residual stress are greatly reduced. The elastic springback finally redistributes the residual stress to an equilibrium state and further reduces the maximum stress value to 5.39MPa.

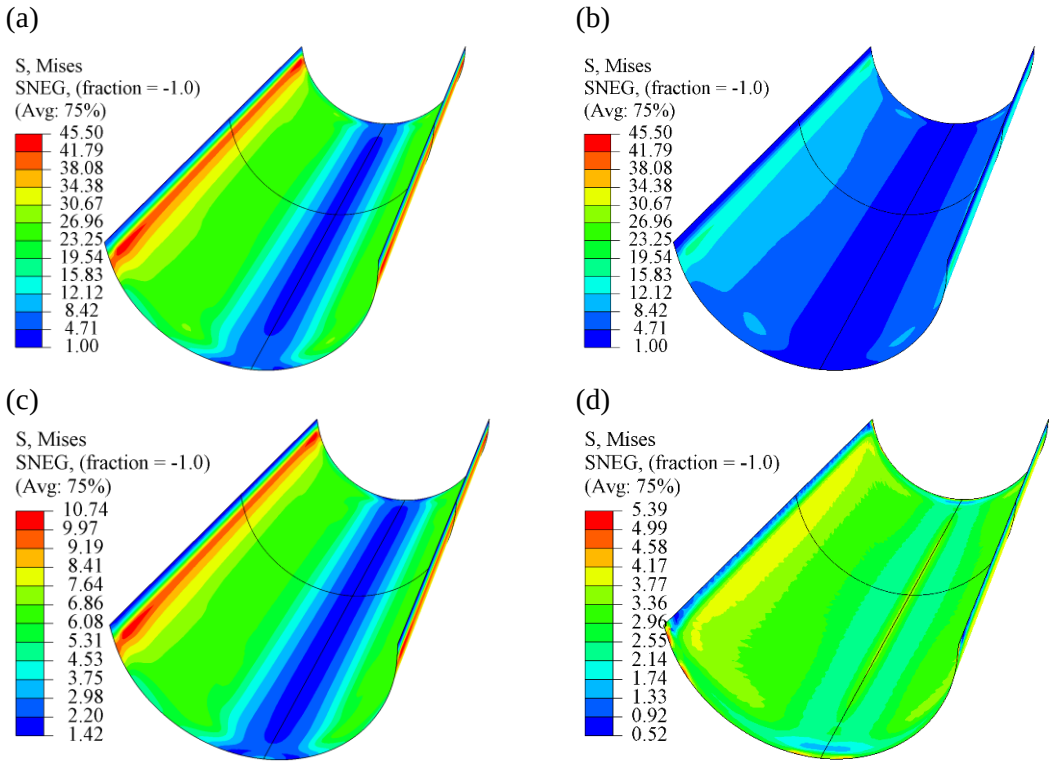

Figure 9. Stress distribution during stress-relaxation and springback at (a) 30s, (b) 2mins, (c) 5mins and (d) after springback.

A series of predicted shapes under different stress-relaxation time and the actual forming shape under 5 min stress-relaxation time from experiments are compared in figure 10. The results show that there is only a tiny difference between the experimental results and corresponding predicted result. This error may come from the determination of constitutive parameters and variation of elastic modulus[25]. It can also be seen from the figure 10 that the stress-relaxation time has a great impact on the accuracy of the formed part.

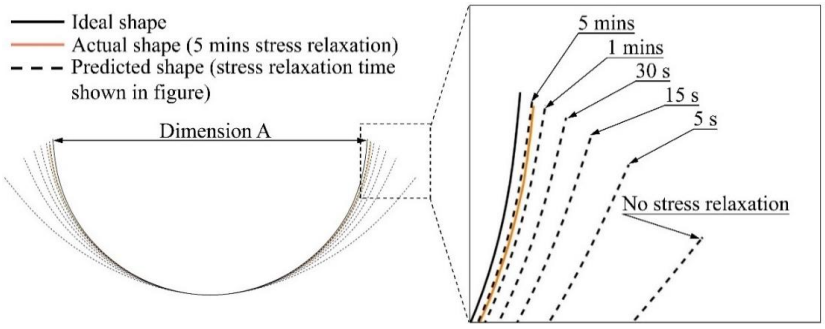

Figure 10. Predicted shapes at different stress-relaxation time and the actual forming shape from experiment with 5min stress-relaxation time.

The size of opening in the formed part, shown as dimension A in figure 10, is used to characterize the shape of these parts, and springback quantity is defined as $(A_{actual} - A_{ideal})/A_{ideal}$. All A dimensions are measured on the neutral surface of the sheet. Figure 11 demonstrates the variation of springback with respect to stress-relaxation time. The amount of springback decreases rapidly within 1 minutes and then almost flattens out in 2 minutes. The prediction error between experiments and modelling results for 5 minutes stress-relaxation condition is only 0.12%. It can be observed that the springback is controlled within 3% after 2 minutes and will not change significantly after 5minutes.

Hence, a stress-relaxation time of 2 to 5 minutes could be reasonable for the isothermal hot stamping process for industrial applications.

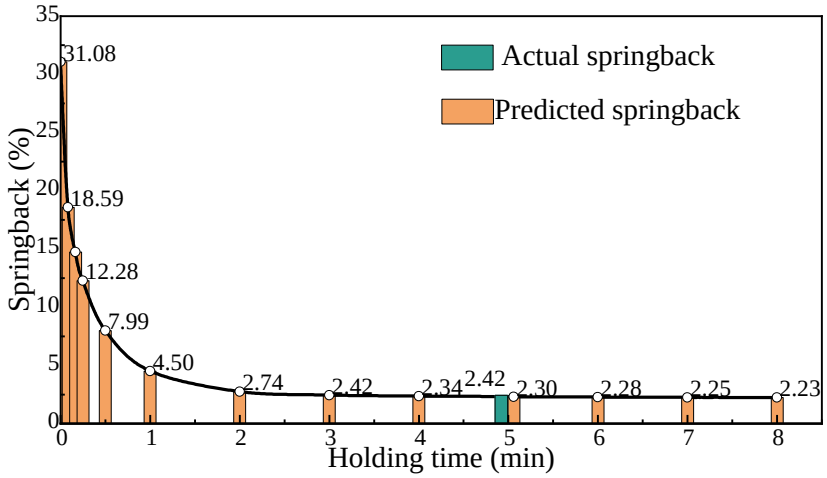

Figure 11. Predicted springback at different stress-relaxation time and the actual springback from experiment at 5min stress-relaxation time.

5. Conclusions

A mechanism-based unified model considering the complete isothermal hot stamping process of plastic deformation and subsequent stress-relaxation steps is developed in this study. This unified model uses the continuous evolution of dislocation density as a medium to link the constitutive relations of these two steps, realizing a continuous description of a complete stamping and stress-relaxation process in isothermal hot stamping process of Ti-6Al-4V.

The unified model is implemented into FE software through subroutines, and an explicit-implicit conjoint simulation process is established for the isothermal hot stamping technology. Comparations between predicted result and actual result of springback of a typical component are done and the prediction error of springback is only 0.12%, proving the developed model to be accurate and effective.

The stress-relaxation step in isothermal hot stamping of Ti-6Al-4V can greatly reduce the residual stress, and improve the forming accuracy greatly. The stress-relaxation time is recommended to be 2 to 5 minutes when the forming temperature is 750℃, while a stress-relaxation step less than 2 minutes cannot fully release the stress and holding time after 5 minutes will not lead to significant improvement of springback.

References

[1] Kopec M 2020 *Hot stamping of titanium alloys* Doctor (Imperial College London)
[2] Vanderhasten M, Rabet L and Verlinden B 2007 Deformation mechanisms of Ti-6Al-4V during tensile behavior at low strain rate *J. Mater. Eng. Perform.* **16** 208–12
[3] Tao Z, Fan X, Yang H, Ma J and Li H 2018 A modified Johnson–Cook model for NC warm bending of large diameter thin-walled Ti–6Al–4V tube in wide ranges of strain rates and temperatures *Trans. Nonferrous Met. Soc. China* **28** 298–308
[4] Lee W-S and Lin C-F 1998 High-temperature deformation behaviour of Ti6Al4V alloy evaluated by high strain-rate compression tests *J. Mater. Process. Technol.* **75** 127–36
[5] Jha J S, Tewari A, Mishra S and Toppo S 2017 Constitutive relations for Ti-6Al-4V hot working *Procedia Eng.* **173** 755–62
[6] Porntadawit J, Uthaisangsuk V and Choungthong P 2014 Modeling of flow behavior of Ti–6Al–4V alloy at elevated temperatures *Mater. Sci. Eng. A* **599** 212–22
[7] Lin J and Liu Y 2003 A set of unified constitutive equations for modelling microstructure evolution in hot deformation *J. Mater. Process. Technol.* **143–144** 281–5

[8] Lin J 2003 Selection of material models for predicting necking in superplastic forming *Int. J. Plast.* **19** 469–81
[9] Lin J and Dean T A 2005 Modelling of microstructure evolution in hot forming using unified constitutive equations *J. Mater. Process. Technol.* **167** 354–62
[10] Garrett R P, Lin J and Dean T A 2005 An investigation of the effects of solution heat treatment on mechanical properties for AA 6xxx alloys: experimentation and modelling *Int. J. Plast.* **21** 1640–57
[11] Li Y, Yu L, Zheng J, Guan B and Zheng K 2021 A physical-based unified constitutive model of AA7075 for a novel hot forming condition with pre-cooling *J. Alloys Compd*. **876** 160142
[12] Zheng K, Li Y, Yang S, Fu K, Zheng J, He Z and Yuan S 2020 Investigation and modeling of the preheating effects on precipitation and hot flow behavior for forming high strength AA7075 at Elevated Temperatures *J. Manuf. Mater. Process.* **4** 76
[13] Meyers M A and Chawla K K 2008 *Mechanical Behavior of Materials* (Cambridge University Press)
[14] Junjie X, Dongsheng L and Xiaoqiang L 2015 Modeling and simulation for the stress relaxation behavior of Ti-6Al-4V at medium temperature *Rare Met. Mater. Eng.* **44** 1046–51
[15] Luo J, Xiong W, Li X and Chen J 2019 Investigation on high-temperature stress relaxation behavior of Ti-6Al-4V sheet *Mater. Sci. Eng.* A **743** 755–63
[16] Rong Q, Shi Z, Li Y and Lin J 2021 Constitutive modelling and its application to stress-relaxation age forming of AA6082 with elastic and plastic loadings *J. Mater. Process.Technol.* **295** 117168
[17] Zhan L, Lin J, Dean T A and Huang M 2011 Experimental studies and constitutive modelling of the hardening of aluminium alloy 7055 under creep age forming conditions *Int. J. Mech. Sci.* **53** 595–605
[18] Li Y, Shi Z, Lin J, Yang Y-L, Rong Q, Huang B-M, Chung T-F, Tsao C-S, Yang J-R and Balint D S 2017 A unified constitutive model for asymmetric tension and compression creep-ageing behaviour of naturally aged Al-Cu-Li alloy *Int. J. Plast.* **89** 130–49
[19] Babu B and Lindgren L-E 2013 Dislocation density based model for plastic deformation and globularization of Ti-6Al-4V *Int. J. Plast.* **50** 94–108
[20] Yang L, Li N, Wang B, Lin J, Zhao H and Ma W 2016 Unified constitutive modelling for two-phase lamellar titanium alloys at hot forming conditions *Manuf. Rev.* **3** 14
[21] Mohamed M S, Foster A D, Lin J, Balint D S and Dean T A 2012 Investigation of deformation and failure features in hot stamping of AA6082: Experimentation and modelling *Int. J. Mach. Tools Manuf.* **53** 27–38
[22] Li K *Thermo-mechanical coupling Numerical simulation of hot stretch bending of titanium alloy sheet* Master (Yanshan University)
[23] Li B, Lin J and Yao X 2002 A novel evolutionary algorithm for determining unified creep damage constitutive equations *Int. J. Mech. Sci.* **44** 987–1002
[24] Cao J and Lin J 2008 A study on formulation of objective functions for determining material models *Int. J. Mech. Sci.* **50** 193–204
[25] Yang X, Dang L, Wang Y, Zhou J and Wang B 2020 Springback prediction of TC4 titanium alloy V-bending under hot stamping condition *J. Cent. South Univ*. **27** 2578–91

Acknowledgments
The research in this paper was funded by the Aeronautical Science Foundation of China (No. 20200036025002), National Natural Science Foundation of China (52005020) and Guangdong Basic and Applied Basic Research Foundation (2019A1515110851)